Published in final edited form as:
J Med Chem. 2009 June 11; 52(11): 3539–3547. doi:10.1021/jm900116d.

Structure-activity relationship of cyanine tau aggregation inhibitors

Edward Chang[†], **Erin E. Congdon**[‡], **Nicolette S. Honson**[†], **Karen E. Duff**[‡], and **Jeff Kuret**[†,*]

[†]Center for Molecular Neurobiology, Department of Molecular and Cellular Biochemistry, The Ohio State University College of Medicine, Columbus, Ohio, USA

[‡]Taub Institute / Department of Pathology, Columbia University and Dept of Integrative Neuroscience, New York State Psychiatric Institute, New York, USA

Abstract

A structure-activity relationship for symmetrical cyanine inhibitors of human tau aggregation was elaborated using a filter trap assay. Antagonist activity depended on cyanine heterocycle, polymethine bridge length, and the nature of meso- and N-substituents. One potent member of the series, 3,3'-diethyl-9-methylthiacarbocyanine iodide (compound **11**), retained submicromolar potency and had calculated physical properties consistent with blood-brain barrier and cell membrane penetration. Exposure of organotypic slices prepared from JNPL3 transgenic mice (which express human tau harboring the aggregation prone P301L tauopathy mutation) to compound **11** for one week revealed a biphasic dose response relationship. Low nanomolar concentrations decreased insoluble tau aggregates to half those observed in slices treated with vehicle alone. In contrast, high concentrations (≥300 nM) augmented tau aggregation and produced abnormalities in tissue tubulin levels. These data suggest that certain symmetrical carbocyanine dyes can modulate tau aggregation in the slice biological model at concentrations well below those associated with toxicity.

Introduction

Alzheimer's disease (AD) is defined in part by the accumulation of aggregated tau proteins within neuronal cell bodies and processes.[1, 2] Because tau aggregate formation correlates with cognitive decline and neurodegeneration,[3, 4] inhibitors of aggregation are under investigation as a means of controlling pathogenesis and preserving neuronal function in disease.[5] Several inhibitory scaffolds capable of supporting tau aggregation antagonist activity *in vitro* have been identified for this purpose, including (but not limited to) phenothiazine,[6] triarylmethane,[7] acridine,[8] phenazine,[8] xanthene,[8] and thiacarbocyanine[9] derivatives. All are polymethine members of the broad π-delocalized lipophilic cation (DLC) family that passively cross cell membranes and accumulate intracellularly depending in part on membrane polarization.[10] A Phase II clinical trial completed with one phenothiazine having aggregation antagonist activity, Methylene blue (3,7-bis(dimethylamino)phenothiazin-5-ium chloride), reported decreased cognitive decline, improved cerebral blood flow, and improved fluorodeoxyglucose uptake relative to placebo over a ~1 year treatment period.[11] Thus at least one tau aggregation antagonist may have therapeutic utility for AD. However, the actions of Methylene blue *in vivo* are not limited to antagonism of tau aggregation. Methylene blue efficiently enters into cyclic redox reactions, during which it is reversibly reduced to Leucomethylene blue,[12] and this cycling may contribute to its biological activity.[13] Thus while Methylene blue is an oxidant

*To whom correspondence should be addressed. Jeff Kuret, OSU Center for Molecular Neurobiology, 1060 Carmack Rd, Columbus, OH 43210, USA, Phone: (614) 688-5899, Fax: (614) 292-5379, E-mail: kuret.3@osu.edu.

capable of modulating the activity of both heme- and non-heme containing enzymes (including nitric oxide synthase[14]), Leucomethylene blue has antioxidant activity and is the active form of the dye during treatment of methemoglobinemia.[15] Moreover, as a DLC, Methylene blue accumulates in mitochondria where it and its reduced form may exert antioxidant effects through interactions with resident electron transport chains.[12] It is not clear whether the therapeutic benefits of Methylene blue stem from its aggregation antagonist activity, its antioxidant effects in mitochondria, its redox modulation of iron-containing proteins, or from other effects.

Recently we introduced thiacarbocyanines as structurally distinct members of the DLC family possessing tau aggregation antagonist activity.[9] The scaffold has several advantages for validating tau aggregation as a therapeutic target. First, certain symmetrical thiacarbocyanines, such as N744 (compound **1**), are among the most potent tau aggregation inhibitors yet described *in vitro*, with submicromolar IC_{50} under near physiological buffer conditions and tau concentrations.[9] Second, because cyanines lack an electron sink analogous to the thiomorpholine ring of Methylene blue, they have much lower reduction potentials[16] and do not enter readily into cycling redox reactions. Third, many carbocyanine derivatives have been prepared over the years, offering a facile route to building SARs. Finally, as with other DLCs, carbocyanine dyes are readily taken up and concentrated in cells where they can contact tau. On the other hand, carbocyanines also present special handling difficulties. First, they are the quintessential aggregation-prone dyes, and readily form face-to-face dimers and higher order aggregates at low concentration.[17] Dye aggregation is a major cause of nonspecific inhibitory effects on unrelated biological targets,[18] which can complicate target validation. Second, many carbocyanines form stable complexes with DNA at micromolar concentrations through groove binding[19] and at high concentrations (~100 μM) through direct intercalation.[20] These interactions could potentially lead to genotoxicity through frameshift mutagenesis or chromosome breakage. Finally, carbocyanines inhibit various enzymes including DNA primase[21] and electron transport complex I (NADH-ubiquinone reductase) of mitochondria.[22-24] Any or all of these actions may contribute to the cytoxicity reported with carbocyanine exposure, including collapse of the microtubule cytoskeleton[25] and induction of apoptosis.[21, 26]

Here we identify the structural features of carbocyanine dyes responsible for tau aggregation inhibitory activity, and demonstrate the activity of one family member in organotypic slice culture. The results suggest potent inhibition of tau aggregation can be achieved *in vitro* and in the biological model at low nanomolar concentrations. Furthermore, bioactivity can be separated from dye aggregation. The results suggest that carbocyanines may have utility for validating tau aggregation as a therapeutic target for AD.

Results

In vitro Activity

Symmetrical carbocyanine dyes consist of two identical heterocycles connected by a polymethine bridge (*i.e*., by a system of conjugated double bonds) (Table 1). Each heterocycle contains an alkyl N-substituent, whereas the bridge can contain hydrogen or other substituents (Table 1). To determine the contribution of these four structural components to tau aggregation antagonist activity, a small library of dyes was subjected to a filter binding assay for ODS-induced fibrillization of human 2N4R tau under near physiological conditions of pH, ionic strength, and reducing conditions. The first series (**2** – **5**, Table 1) evaluated the influence of polymethine bridge length on inhibitory activity. Bridge length influences the photophysical properties of cyanine dyes[27] and is a major determinant of molecule length. The series contained identical ethyl N-substituents, only hydrogen bridge substituents, and two benzothiazole heterocycles, whereas the polymethine bridge was systematically varied in

length from zero to three methine units (*i.e*., the bridges varied from one to seven carbons in length) (Table 1). All four compounds inhibited tau aggregation but with weaker potencies than starting compound **1** (Figure 1A). A replot of IC_{50} versus polymethine bridge length revealed a clear optimum centered on a bridge length of three carbons (Figure 1B). Therefore, further studies were limited to compounds containing a polymethine bridge of this length.

To evaluate the contribution of heterocycle composition, the second series (**3, 6, 7**, and **8**) contained ethyl N-substituents and a hydrogen meso group in the presence of either benzothiazole, benzoxazole, dimethylindole, or quinoline heterocycles. Heterocycle composition influences compound polarizability and also ability to form H-bonds with solvent.[28] All heterocycles were as potent and efficacious as benzothiazole **3** except benzoxazole **6**, which had essentially no inhibitory activity at the highest concentration tested (Figure 2). These data show that inhibitory activity is not uniquely associated with the benzothiazole heterocycle, and can be extended to other heterocycles lacking sulfur.

Cyanine N-substituents consist of alkyl or other groups (including ionizable groups) that do not participate in extended conjugated bond structure. Nonetheless, substituent structure influences compound pharmacokinetics by modulating binding affinity for serum albumin[29] and by affecting net compound charge (and hence ability to serve as substrates for organic anion/cation transporters[30]). The contribution of N-substituent to inhibitory activity was evaluated in both benzothiazole and dimethylindole heterocycle-containing dyes. In the dimethylindole background, elongation of the alkyl chains from two carbons (**8**) to three carbons (**9**) reduced inhibitory potency ~3-fold (Figure 3). In a benzothiazole background, elongation of the alkyl chains from two carbons (**3**) to six carbons (**10**) completely eliminated activity at up to 10 μM concentration (Figure 3). These data indicate that short N-alkyl substituents are most compatible with inhibitory activity.

Finally, the contribution of the meso substituent was investigated. Meso groups modulate the configuration of the polymethine bridge, with a hydrogen substituent favoring s-trans conformation whereas larger substituents favor s-cis conformation.[31] The addition of a methyl meso substituent (**11**) retained efficacy while decreasing IC_{50} 3-fold to ~300 nM (Figure 3). These data indicated that s-cis conformation was most compatible with inhibitory activity. Nonetheless, the beneficial effects of meso substitution were completely lost at all concentrations up to 10 μM when N-substituents were replaced with sulfonated propyl moieties (**12**) (Figure 3). Similarly, enlargement of the heterocycle to naphthothiazole in the presence of a methyl meso group (**13**) did not further increase potency above that attained with the benzothiazole heterocycle (Figure 3).

The SAR for symmetrical cyanine dyes summarized above indicates that it is possible to retain the potency and efficacy of parent compound **1**, but with molecular weight, calculated octanol:water partition coefficient (ClogP), and topological polar surface area (tPSA) values more consistent with potential CNS penetration[32] (Table 1). To confirm these findings, the most potent compound in the cyanine series (**11**) was assayed by an independent method (quantitative electron microscopy) and compared to established inhibitor Methylene blue. Results showed that the efficacy and potency of **11** was consistent in both filter trap and electron microscopy assay formats (Figure 4). In comparison, Methylene blue behaved as a partial antagonist with an IC_{50} of 610 ± 50 nM. These data indicate that cyanine inhibitors with superior *in silico* physical properties are available that exceed the potency and efficacy of Methylene blue *in vitro*.

Dye Aggregation

Many planar heterocycles aggregate depending on pH, ionic strength, temperature, solvent polarity, and compound concentration.[33] Symmetrical carbocyanine dyes are especially

aggregation prone in water owing to strong dispersion forces between their nearly planar faces[34] and H-bond formation with solvent.[28] Shifts in absorbance spectra accompany thiacarbocyanine aggregation depending on the quaternary structure of the aggregate formed. Hypsochromic shifts to shorter wavelengths are generally referred to as H-bands.[35] In solution, these correspond primarily to small aggregates (*e.g.*, dimer) although much larger sizes can be attained at high concentration or in the presence of certain surfaces.[36] In previous studies, formation of large H-aggregates correlated with loss of **1** inhibitory activity.[17] However, substantial amounts of H-dimer were present at inhibitory concentrations suggesting these were candidate inhibitory species. To test this hypothesis, the concentration dependent aggregation of the carbocyanine dye series shown in Table 1 was assessed by absorbance spectroscopy and compared to the SAR for tau aggregation inhibition. In neat methanol (which does not support dye oligomerization[27]), **11** absorbance appeared as a major band at 544 nm with a weak vibrational shoulder at ~510 nm (Figure 5A). At low micromolar concentration in aqueous solution (*i.e.*, assembly buffer), monomer appeared centered at 541 nm, consistent with the solvatochromic behavior of many thiacarbocyanine derivatives.[37] As **11** concentration increased, a second absorbance maximum centered at 502 nm also became apparent. On the basis of absorption spectra of other thiacarbocyanine dyes,[27] the 502 nm band corresponds to an H-dimer (Figure 5A). To confirm this prediction, the amount of monomer as a function of bulk **11** concentration was determined by absorbance spectroscopy and used to calculate the concentration of putative dimer by use of eq 1. A double log plot of monomer *versus* dimer concentration was linear with a slope of 2.3 ± 0.1, confirming that the reaction was consistent with dimerization (Figure 6). On the basis of eq 3, the dissociation equilibrium constant for dimerization (K_{dim}) was 20.9 ± 0.7μM. Thus, **11** readily dimerizes at low micromolar concentrations under near physiological buffer conditions, but at 10.0 ± 0.2-fold higher concentrations than **1** under identical conditions.[38] These data suggest that dimerization can be dissociated from inhibitory activity. Indeed, certain cyanines with weak or no inhibitory activity, such as **5** (K_{dim} = 0.68 ± 0.04 μM) and **12** (K_{dim} = 7.5 ± 0.4 μM) dimerized more efficiently than **11** (Figs. 5B and 6). Conversely, other compounds, such as dimethylindocarbocyanine **8**, inhibited tau aggregation at micromolar concentrations (Table 1) but did not dimerize at any concentration tested up to 96 μM (Figure 5C). Overall, there was no discernible correlation between dimerization propensity of compounds listed in Table 1 and inhibitory potency, suggesting that the active inhibitory species in the low concentration regime is the cyanine monomer.

Biological Activity

The *in vitro* SAR described above suggests that cyanine dyes should inhibit tau aggregation in biological models at sub-micromolar concentrations. To test this prediction, organotypic slices prepared from JNPL3 transgenic mice were exposed to a broad concentration range (0.1 nM – 1 μM) of **11** over a period of seven days after which levels of sarkosyl-insoluble tau were estimated. Compound **11** was chosen for study because it was the most potent member of the carbocyanine series. The JNPL3 model was selected as host because it accumulates tau aggregates in the diencephalon, brainstem, and cerebellar nuclei and is well characterized.[39-43] The model is driven by expression of tau above normal physiological levels, which leads to increased nucleation and extension rates,[44] and by insertion of the P301L missense mutation, which increases both the rate and extent of aggregation still further compared to wild-type tau protein.[45] The effects of **11** in this model were biphasic (Figure 7AB). In the low concentration regime (1 – 10 nM) the compound decreased tau aggregation to ~50% of that observed in the presence of DMSO vehicle alone. Inhibitory activity was lost at 100 nM, whereas tau aggregation was induced at 300 nM and above.

In cell culture models, >300 nM **11** reportedly initiates apoptosis[21, 26] and collapse of the microtubule cytoskeleton.[25] To determine whether **11** induced similar toxicity in neurons,

organotypic slices exposed to **11** were assayed for changes in levels of cleaved PARP1 (an enzyme that is proteolytically inactivated by caspases during apoptosis)[46] and α-tubulin (the structural component of microtubules). Levels of cleaved PARP1 were low in the presence of vehicle alone and did not increase at any tested concentration of **11**, suggesting that proapoptotic caspases were not activated under these conditions (Fig. 8). Similarly, levels of α-tubulin were unchanged in cultures incubated with concentrations of **11** (1 nM) that inhibited tau aggregation (Fig. 8). However, at high **11** concentrations (1 μM), depletion of α-tubulin from extracts was detected, suggesting misfunction of the microtubule cytoskeleton under these conditions (Fig. 8). Together these data indicate that a cyanine identified on the basis of *in vitro* methods can modulate tau aggregation in a biological model, and is effective at concentrations well below those associated with toxicity in the form of induction of apoptosis or misfunction of the microtubule cytoskeleton.

Discussion

Despite promising effects reported for Methylene blue on AD progression, the significance of tau aggregation as a therapeutic target requires further validation. The SAR summarized above suggests that cyanine dyes may have utility for this purpose. In particular, the availability of active and inactive cyanines sharing very similar structure will help clarify whether direct (herein) or indirect[47] mechanisms mediate clearance of tau aggregates in biological models.

Both cyanines and Methylene blue consist of strong electron donor and acceptor substituents separated by a conjugated bridge composed of an odd number of carbon atoms. This organization supports the ideal polymethine state characterized by alternating π-electron density distribution along the molecular chain and by high polarizability.[48] These properties may be important for tau aggregation inhibitory activity. Consistent with this hypothesis, the benzoxazole heterocycle, which had the lowest polarizability in the series (owing to the electronegative oxygen atom at position X; Table 1) lacked inhibitory activity. Polarizability also gives rise to strong dispersion forces that support efficient compound self association.[48] However, as reported previously for a macrocyclic thiacarbocyanine,[49] and through SAR here, the propensity for face-to-face association can be separated from inhibitory activity. Dimethylindocyanines, which contain geminal methyl groups that interfere with ordered stacking even in the presence of templates such as DNA,[50] offer a scaffold that is particularly dimerization resistant. Elimination of stacking interactions with itself or with DNA may be important for limiting potential toxicity associated with chronic cyanine exposure.

One symmetrical carbocyanine, indocyanine green (**14**; Table 1), is approved for diagnostic applications,[51, 52] but its molecular properties are not appropriate for tau aggregation inhibitor activity. In particular, its high molecular weight precludes efficient uptake into CNS, and its extended polymethine bridge, long sulfonated N-substituents, and hydrophobic benzindole heterocycles, confer tight binding to serum albumin. As a result, **14** resides primarily in blood plasma after administration.[53] In contrast, the molecular properties associated with cyanine aggregation antagonists are predicted to support better CNS bioavailability than currently possible with **14**. Nonetheless, it will be necessary to address the short half-life of cyanines in plasma. For example, compound **14** is rapidly cleared unchanged through the hepatobiliary route.[54] It enters hepatocytes through organic anion-transporting polypeptides in the sinusoidal (basolateral) membrane, and is excreted through the canalicular (apical) membrane through the P-glycoprotein efflux transporter.[55] Other cyanines, such as **6**, share affinity for this efflux transporter,[56] but not necessarily the passive transporters in the sinusoidal membrane owing to differences in net charge. Chemical strategies for decreasing the rate of **14** hepatic clearance are under investigation[57] and may be applicable to tau aggregation inhibitors as well.

Compound **11** inhibited tau aggregation in organotypic slices at media concentrations as low as 1 nM. This high apparent potency may arise from several considerations. First, DLCs including cyanine dyes are readily taken up and concentrated in cells and tissues. For example, cultured K562 cells (a human erythroleukemic cell line established from a patient with chronic myelogenous leukemia in blast transformation) reportedly accumulate intracellular indo-, thia-, and oxo-carbocyanines two orders of magnitude over applied concentrations in media.[58] These cells accumulate DLCs because their mitochondrial membrane potentials are hyperpolarized relative to non-transformed cells[10, 59] and because they lack the P-glycoprotein efflux transporter.[60] Second, cytoplasmic DLCs accumulate near membranes, which are putative sites of tau filament nucleation.[61, 62] Thus, compound concentrations at local intracellular sites of action may be far higher than implied solely on the basis of bulk concentrations in media.

Compound uptake into organotypic brain slices may follow similar principles. In brain, the P-glycoprotein efflux transporter is predominantly located on the luminal membrane of endothelial cells lining brain microvessels associated with the blood-brain barrier. The slice preparation bypasses this barrier and facilitates direct exposure of neurons undergoing tau aggregation to compounds. Because neurons do not express P-glycoprotein under basal conditions,[63] the slice preparation is particularly useful for assessing the activity of cyanines in neurons until analogs with improved pharmacokinetics are available.

In summary, symmetrical carbocyanines are more potent tau aggregation antagonists than Methylene blue. Their structures are consistent with favorable *in silico* pharmacokinetic predictions, whereas confounding activities such as dye aggregation, DNA intercalation, and high affinity serum albumin binding can be attenuated without destroying inhibitory potency. Therefore, these compounds may have utility for target validation. Organotypic slices prepared from transgenic mouse models will help this effort. In particular, their ability to support robust aggregation over a period of weeks while preserving CNS organization is ideally suited to development of intracellular protein aggregation antagonists.

Experimental Section

Materials

Recombinant His-tagged wild-type 2N4R tau (*i.e.*, the longest human central nervous system isoform of tau[64]) was prepared as described previously.[65] Mouse monoclonal antibodies Tau5[66] and CP27[67] were gifts from L.I. Binder (Northwestern University, IL) and P. Davies (Albert Einstein College of Medicine, NY), respectively, whereas rabbit polyclonal anti-cleaved PARP1 and mouse monoclonal anti-α-tubulin antibodies were from Cell Signaling (Danvers, MA) and Sigma-Aldrich (St. Louis, MO), respectively. Nitrocellulose membrane (0.2 μM porosity) was from Bio-Rad Laboratories (Hercules, CA). Protease inhibitors (1× complete contained: 1 mM 4-(2-aminoethyl)-bezenesulfonylfluoride, 0.85 μM aprotinin, 40 μM bestatin, 20 μM leupeptin, 15 μM pepstatin A, 14 μM *trans*-Epoxysuccinyl-L-leucylamido [4- guanidino]butane) were from Sigma-Aldrich. Formvar/carbon-coated copper grids, glutaraldehyde, and uranyl acetate were obtained from Electron Microscopy Sciences (Fort Washington, PA). Aggregation inducer ODS was obtained from Lancaster Synthesis (Pelham, NH) and was dissolved in 1:1 water:isopropanol before use. Screened compounds included **1**[9, 17], cyanines **2** - **13** (Sigma-Aldrich), and Methylene blue (Acros Organics, Morris Plains, NJ). All compounds, which were at least 95% pure on the basis of argentometric titration (**5**), high-performance capillary electrophoresis (**6**), thin-layer chromatography (**8, 9, 10**), or HPLC analysis (all others), were dissolved in DMSO prior to use.

Tau Aggregation *in vitro*

Tau preparations were incubated (37°C) without agitation in assembly buffer (10 mM HEPES, pH 7.4, 100 mM NaCl, 5 mM dithiothreitol) for 24 h in the presence or absence of fibrillization inducer ODS (50 μM) and candidate inhibitors. Control reactions contained DMSO vehicle, which was limited to 1% (v/v) final concentration in all aggregation reactions. After incubation, reactions were immediately assayed by either filter trap assay or electron microscopy as described below.

Filter Trap Assay

This was performed as described previously.[45] Briefly, reactions were diluted in 2% SDS before vacuum filtration in triplicate through a 96-well dot blot apparatus onto nitrocellulose membranes. Membranes were washed twice with 2% SDS, blocked with 4% nonfat dry milk in blocking buffer (100 mM Tris-HCl, pH 7.4, and 150 mM NaCl) for 2 h, and incubated with Tau5 primary antibody for 1.5 h. They were then washed twice in blocking buffer and then incubated with HRP-linked secondary antibody for 1.5 h. The membranes were washed again in blocking buffer and developed with the ECL (Enhanced Chemiluminescence) Western Blotting Analysis System (GE Healthcare, Buckinghamshire, UK). Chemiluminescence was recorded on an Omega 12iC Molecular Imaging System and quantified using UltraQuant software (UltraLum, Claremont, CA) and is reported ± SD.

Electron Microscopy

Reaction aliquots were removed, treated with 2% glutaraldehyde (final concentration), mounted on formvar/carbon-coated 300 mesh grids, and negatively stained with 2% uranyl acetate as described previously.[68] Random fields were viewed with a Tecnai G2 Spirit BioTWIN transmission electron microscope (FEI, Hillsboro, OR) operated at 80kV and 23,000-49,000× magnification. At least three viewing fields were captured for each reaction condition and filaments >10 nm in length were counted and quantified with ImageJ software (National Institutes of Health, Bethesda, MD). Total filament length is defined as the sum of the lengths of all resolved filaments per field and is reported as ± SD.

Dye Aggregation

Compounds were incubated (1 h at 37°C) in assembly buffer, then subjected to absorbance spectroscopy (Varian Cary 50 Bio) over the wavelength range 400 - 700 nm. Concentrations of dye monomer (C_m) were estimated as described previously.[27, 38] Briefly, the extinction coefficient for dye monomer was established in methanol, and then used to estimate monomer concentration in aqueous solutions on the basis of the Beer-Lambert law:

$$A=\varepsilon C_m l \quad (1)$$

where A is absorbance, ε is the molar extinction coefficient, and l is the path length of the sample. Dimer concentration (C_d) was estimated from total dye concentration (C_t) assuming:[27]

$$C_d=(C_t C_m)/2 \quad (2)$$

The dissociation constant for dimerization (K_{dim}) was then calculated from the function:[27]

$$K_{\mathrm{dim}}=C_{\mathrm{m}}^{2}/C_{\mathrm{d}} \quad (3)$$

K_{dim} values were derived from at least five spectra and reported as mean ± S.D.

Organotypic Slice Culture

Brains were harvested from JNPL3 mice[40] at postnatal day ten. After removal of cerebellum and brainstem, the cerebral cortex and hippocampus were sectioned at 400 μm as described previously.[69] Slices from each hemisphere were then separated in ice cold buffer (pH 7.1), transferred to membrane inserts containing 0.4 μm pores (Laboratory Disposable Products; Wayne, NJ), and then maintained in culture for 14 days in media containing 25% serum (media was changed every two days). After the culture period, slices prepared from one hemisphere were treated with varying concentrations of compound for seven days, whereas slices prepared from the contralateral hemisphere were treated with DMSO vehicle alone (0.008% final concentration of DMSO in media). Thus, the vehicle-treated hemispheres served as within-animal controls for each treatment condition.

Tissue fractionation

Treated and control slices were separately pooled and homogenized by sonication in cold RIPA buffer (50 mM Tris-HCl, pH 7.4, 150 mM NaCl, 1 mM EDTA, 1 mM NaF, 1 mM Na_3VO_4, 1× protease inhibitors, 1μg/mL phosphatase inhibitors).[70] Homogenates were then centrifuged at 20,000*g* at 4°C for 20 min. The resulting supernatant fractions (crude extracts) were collected and assayed for α-tubulin and cleaved PARP1 immunoreactivity using a Fujifilm LAS3000 imaging system.

To assess tau aggregation, extracts were diluted in RIPA buffer as necessary to achieve equivalent total protein levels. An aliquot of low-speed supernatant was incubated in 1% sarkosyl for 30 min at room temperature. Samples were then centrifuged for 1 h at 100,000*g* at 20°C. Supernatant was discarded and the pellet, termed the sarkosyl-insoluble fraction, was then resuspended in 20 μL O+ buffer (a modified O buffer[71] composed of 62.5 mM Tris-HCl, pH 6.8, 10% glycerol, 5% 2-mercaptoethanol, 2.3% SDS, 1 mM EGTA, 1 mM EDTA, 1 mM PMSF, 1 mM Na_3VO_4, 1 mM NaF, 1× protease inhibitors), boiled for 3 min, then subjected to immunoblot analysis using monoclonal antibody CP27.

Analytical Methods

Concentration effect data from either filter or electron microscopy assays were normalized to DMSO vehicle control reactions and fit to the function:

$$y=y_{\mathrm{min}}+\frac{y_{\mathrm{max}}-y_{\mathrm{min}}}{\left(1+10^{(\log IC_{50}-\log x)n}\right)} \quad (4)$$

where y and y_{max} represent the minimum and maximum aggregation measured in the presence and absence of inhibitor (at concentration x), respectively, n is the Hill coefficient, and IC_{50} is the concentration of inhibitor that results in 50% of maximal inhibition. IC_{50} values are reported ± standard error of the estimate.

Acknowledgments

We thank Dr. Jeremy D. Pettigrew, Ohio State University Department of Chemistry, for helpful discussions. This work was supported by National Institutes of Health grants NS047447 (K.E.D.) and AG14452 (J.K.).

References

1. Ballatore C, Lee VM, Trojanowski JQ. Tau-mediated neurodegeneration in Alzheimer's disease and related disorders. Nat Rev Neurosci 2007;8:663–672. [PubMed: 17684513]
2. Buee L, Bussiere T, Buee-Scherrer V, Delacourte A, Hof PR. Tau protein isoforms, phosphorylation and role in neurodegenerative disorders. Brain Res Brain Res Rev 2000;33:95–130. [PubMed: 10967355]
3. Congdon EE, Duff KE. Is tau aggregation toxic or protective? J Alzheimers Dis 2008;14:453–457. [PubMed: 18688098]
4. Honson NS, Kuret J. Tau aggregation and toxicity in tauopathic neurodegenerative diseases. J Alzheimers Dis 2008;14:417–422. [PubMed: 18688092]
5. Kuret, J. Detection and Reduction of Neurofibrillary Lesions. In: Smith, HJ.; Sewell, RDE.; Simons, C., editors. Protein Folding Diseases: Enzyme Inhibitors and Other Agents as Prospective Therapies. Vol. 5. CRC Press, Taylor & Francis Books; Boca Raton, FL: 2007. p. 287-324.
6. Wischik CM, Edwards PC, Lai RY, Roth M, Harrington CR. Selective inhibition of Alzheimer disease-like tau aggregation by phenothiazines. Proc Natl Acad Sci U S A 1996;93:11213–11218. [PubMed: 8855335]
7. Honson NS, Johnson RL, Huang W, Inglese J, Austin CP, Kuret J. Differentiating Alzheimer disease-associated aggregates with small molecules. Neurobiol Dis 2007;363:229–234.
8. Wischik, CM.; Edwards, PC.; Harrington, CR.; Roth, M.; Klug, A. Inhibition of tau-tau association. U S Patent. 6,953,794. 2005.
9. Chirita CN, Necula M, Kuret J. Ligand-Dependent Inhibition and Reversal of Tau Filament Formation. Biochemistry 2004;43:2879–2887. [PubMed: 15005623]
10. Modica-Napolitano JS, Aprille JR. Delocalized lipophilic cations selectively target the mitochondria of carcinoma cells. Adv Drug Deliv Rev 2001;49:63–70. [PubMed: 11377803]
11. Wischik, CM.; Bentham, P.; Wischik, DJ.; Seng, KM. Tau aggregation inhibitor (TAI) therapy with rember$^{(tm)}$ arrests disease progression in mild and moderate Alzheimer's disease over 50 weeks. 11th International Conference on Alzheimer's Disease; Chicago, IL. 2008.
12. Atamna H, Nguyen A, Schultz C, Boyle K, Newberry J, Kato H, Ames BN. Methylene blue delays cellular senescence and enhances key mitochondrial biochemical pathways. FASEB J 2008;22:703–712. [PubMed: 17928358]
13. Buchholz K, Schirmer RH, Eubel JK, Akoachere MB, Dandekar T, Becker K, Gromer S. Interactions of methylene blue with human disulfide reductases and their orthologues from Plasmodium falciparum. Antimicrob Agents Chemother 2008;52:183–191. [PubMed: 17967916]
14. Mayer B, Brunner F, Schmidt K. Inhibition of nitric oxide synthesis by methylene blue. Biochem Pharmacol 1993;45:367–374. [PubMed: 7679577]
15. Yusim Y, Livingstone D, Sidi A. Blue dyes, blue people: the systemic effects of blue dyes when administered via different routes. J Clin Anesth 2007;19:315–321. [PubMed: 17572332]
16. Zigman S, Gilman P Jr. Inhibition of cell division and growth by a redox series of cyanine dyes. Science 1980;208:188–191. [PubMed: 7361115]
17. Congdon EE, Necula M, Blackstone RD, Kuret J. Potency of a tau fibrillization inhibitor is influenced by its aggregation state. Arch Biochem Biophys 2007;465:127–135. [PubMed: 17559794]
18. Feng BY, Simeonov A, Jadhav A, Babaoglu K, Inglese J, Shoichet BK, Austin CP. A High-Throughput Screen for Aggregation-Based Inhibition in a Large Compound Library. J Med Chem 2007;50:1385–2390.
19. Hannah KC, Armitage BA. DNA-templated assembly of helical cyanine dye aggregates: a supramolecular chain polymerization. Acc Chem Res 2004;37:845–853. [PubMed: 15612674]

20. Biver T, De Biasi A, Secco F, Venturini M, Yarmoluk S. Cyanine dyes as intercalating agents: kinetic and thermodynamic studies on the DNA/Cyan40 and DNA/CCyan2 systems. Biophys J 2005;89:374–383. [PubMed: 15863482]
21. Li ZM, Liu ZC, Guan ZZ, Zhu XF, Zhou JM, Xie BF, Feng GK, Zhu ZY, Jiang WQ. Inhibition of DNA primase and induction of apoptosis by 3,3'-diethyl-9-methylthia-carbocyanine iodide in hepatocellular carcinoma BEL-7402 cells. World J Gastroenterol 2004;10:514–520. [PubMed: 14966908]
22. Anderson WM, Chambers BB, Wood JM, Benninger L. Inhibitory effects of two structurally related carbocyanine laser dyes on the activity of bovine heart mitochondrial and Paracoccus denitrificans NADH-ubiquinone reductase. Evidence for a rotenone-type mechanism. Biochem Pharmacol 1991;41:677–684. [PubMed: 1900156]
23. Anderson WM, Delinck DL, Benninger L, Wood JM, Smiley ST, Chen LB. Cytotoxic effect of thiacarbocyanine dyes on human colon carcinoma cells and inhibition of bovine heart mitochondrial NADH-ubiquinone reductase activity via a rotenone-type mechanism by two of the dyes. Biochem Pharmacol 1993;45:691–696. [PubMed: 8442768]
24. Anderson WM, Wood JM, Anderson AC. Inhibition of mitochondrial and Paracoccus denitrificans NADH-ubiquinone reductase by oxacarbocyanine dyes. A structure- activity study. Biochem Pharmacol 1993;45:2115–2122. [PubMed: 8512593]
25. Lee C, Wu SS, Chen LB. Photosensitization by 3,3'-dihexyloxacarbocyanine iodide: specific disruption of microtubules and inactivation of organelle motility. Cancer Res 1995;55:2063–2069. [PubMed: 7743503]
26. Li ZM, Jiang WQ, Guan ZZ, Zhu XF, Zhou JM, Xie BF, Feng GK, Zhu ZY, Liu ZC. Apoptosis induced by DNA primase inhibitor 3,3'-diethyl-9-methylthia-carbocyanine iodide in human leukemia HL-60 cells. Acta Pharmaceutica Sinica 2006;41:978–984. [PubMed: 17184117]
27. West W, Pearce S. The dimeric state of cyanine dyes. J Phys Chem 1965;69:1894–1903.
28. Vranchev DP, Andreev GN, Staneva TG, Krustev TA. Association processes of some polymethine compounds, studied in relation to their structural peculiarities. Bulg J Phys 1978;5:607–612.
29. Tatikolov AS, Costa SM. Complexation of polymethine dyes with human serum albumin: a spectroscopic study. Biophys Chem 2004;107:33–49. [PubMed: 14871599]
30. Klaassen CD, Lu H. Xenobiotic transporters: ascribing function from gene knockout and mutation studies. Toxicol Sci 2008;101:186–196. [PubMed: 17698509]
31. West W, Pearce S, Grum F. Steroisomerism in Cyanine Dyes-Meso-Substituted Thiacarbocyanines. J Phys Chem 1967;71:1316–1326.
32. Hou TJ, Xu XJ. ADME evaluation in drug discovery. 3. Modeling blood-brain barrier partitioning using simple molecular descriptors. J Chem Inf Comput Sci 2003;43:2137–2152. [PubMed: 14632466]
33. Murakami K. Thermodynamic and kinetic aspects of self-association of dyes in aqueous solution. Dyes and Pigments 2002;53:31–43.
34. Herz, AH. Adsorption of sensititzing dyes to silver halides. In: James, TH., editor. Theory of the photographic Process. Vol. Fourth Edition. Macmillan, Inc; New York, NY: 1977. p. 235-250.
35. Herz AH. Dye-Dye interactions of cyanines in solution and at silver bromide surfaces. Photogr Sci Eng 1974;18:323–335.
36. Maskasky JE. Molecular-orientation of individual J aggregates on gelatin-grown AgBr tabular microcrystals. Langmuir 1991;7:407–421.
37. Seifert JL, Connor RE, Kushon SA, Wang M, Armitage BA. Spontaneous assembly of helical cyanine dye aggregates on DNA nanotemplates. J Am Chem Soc 1999;121:2987–2995.
38. Necula M, Chirita CN, Kuret J. Cyanine dye n744 inhibits tau fibrillization by blocking filament extension: implications for the treatment of tauopathic neurodegenerative diseases. Biochemistry 2005;44:10227–10237. [PubMed: 16042400]
39. Arendash GW, Lewis J, Leighty RE, McGowan E, Cracchiolo JR, Hutton M, Garcia MF. Multi-metric behavioral comparison of APPsw and P301L models for Alzheimer's disease: linkage of poorer cognitive performance to tau pathology in forebrain. Brain Res 2004;1012:29–41. [PubMed: 15158158]

40. Lewis J, McGowan E, Rockwood J, Melrose H, Nacharaju P, Van Slegtenhorst M, Gwinn-Hardy K, Paul Murphy M, Baker M, Yu X, Duff K, Hardy J, Corral A, Lin WL, Yen SH, Dickson DW, Davies P, Hutton M. Neurofibrillary tangles, amyotrophy and progressive motor disturbance in mice expressing mutant (P301L) tau protein. Nat Genet 2000;25:402–405. [PubMed: 10932182]
41. Lin WL, Lewis J, Yen SH, Hutton M, Dickson DW. Ultrastructural neuronal pathology in transgenic mice expressing mutant (P301L) human tau. J Neurocytol 2003;32:1091–1105. [PubMed: 15044841]
42. Lin WL, Lewis J, Yen SH, Hutton M, Dickson DW. Filamentous tau in oligodendrocytes and astrocytes of transgenic mice expressing the human tau isoform with the P301L mutation. Am J Pathol 2003;162:213–218. [PubMed: 12507904]
43. Lin WL, Zehr C, Lewis J, Hutton M, Yen SH, Dickson DW. Progressive white matter pathology in the spinal cord of transgenic mice expressing mutant (P301L) human tau. J Neurocytol 2005;34:397–410. [PubMed: 16902761]
44. Congdon EE, Kim S, Bonchak J, Songrug T, Matzavinos A, Kuret J. Nucleation-dependent tau filament formation: the importance of dimerization and an estimation of elementary rate constants. J Biol Chem 2008;283:13806–13816. [PubMed: 18359772]
45. Chang E, Kim S, Yin H, Nagaraja HN, Kuret J. Pathogenic missense *MAPT* mutations differentially modulate tau aggregation propensity at nucleation and extension steps. J Neurochem 2008;107:1113–1123. [PubMed: 18803694]
46. Oliver FJ, de la Rubia G, Rolli V, Ruiz-Ruiz MC, de Murcia G, Murcia JM. Importance of poly(ADP-ribose) polymerase and its cleavage in apoptosis. Lesson from an uncleavable mutant. J Biol Chem 1998;273:33533–33539. [PubMed: 9837934]
47. Honson NS, Jensen JR, Abraha A, Hall GF, Kuret J. Small-molecule mediated neuroprotection in an in situ model of tauopathy. Neurotox Res 2009;15:274–283. [PubMed: 19384600]
48. Dähne S. Color and Constitution: One Hundred Years of Research. Science 1978;199:1163–1167. [PubMed: 17745588]
49. Honson NS, Jensen JR, Darby MV, Kuret J. Potent inhibition of tau fibrillization with a multivalent ligand. Biochem Biophys Res Commun 2007;363:229–234. [PubMed: 17854770]
50. Garoff RA, Litzinger EA, Connor RE, Fishman I, Armitage BA. Helical aggregation of cyanine dyes on DNA templates: Effect of dye structure on formation of homo- and heteroaggregates. Langmuir 2002;18:6330–6337.
51. Brancato R, Trabucchi G. Fluorescein and indocyanine green angiography in vascular chorioretinal diseases. Semin Ophthalmol 1998;13:189–198. [PubMed: 9878669]
52. Caesar J, Shaldon S, Chiandussi L, Guevara L, Sherlock S. The use of indocyanine green in the measurement of hepatic blood flow and as a test of hepatic function. Clin Sci 1961;21:43–57. [PubMed: 13689739]
53. Meijer DK, Weert B, Vermeer GA. Pharmacokinetics of biliary excretion in man. VI. Indocyanine green. Eur J Clin Pharmacol 1988;35:295–303. [PubMed: 3181282]
54. Cherrick GR, Stein SW, Leevy CM, Davidson CS. Indocyanine green: observations on its physical properties, plasma decay, and hepatic extraction. J Clin Invest 1960;39:592–600. [PubMed: 13809697]
55. Huang L, Vore M. Multidrug resistance p-glycoprotein 2 is essential for the biliary excretion of indocyanine green. Drug Metab Dispos 2001;29:634–637. [PubMed: 11302927]
56. Li M, Yuan H, Li N, Song G, Zheng Y, Baratta M, Hua F, Thurston A, Wang J, Lai Y. Identification of interspecies difference in efflux transporters of hepatocytes from dog, rat, monkey and human. Eur J Pharm Sci 2008;35:114–126. [PubMed: 18639632]
57. Licha K, Riefke B, Ntziachristos V, Becker A, Chance B, Semmler W. Hydrophilic cyanine dyes as contrast agents for near-infrared tumor imaging: synthesis, photophysical properties and spectroscopic in vivo characterization. Photochem Photobiol 2000;72:392–398. [PubMed: 10989611]
58. Sima PD, Kanofsky JR. Cyanine dyes as protectors of K562 cells from photosensitized cell damage. Photochem Photobiol 2000;71:413–421. [PubMed: 10824591]
59. Modica-Napolitano JS, Kulawiec M, Singh KK. Mitochondria and human cancer. Curr Mol Med 2007;7:121–131. [PubMed: 17311537]

60. Marques-Santos LF, Oliveira JG, Maia RC, Rumjanek VM. Mitotracker green is a P-glycoprotein substrate. Biosci Rep 2003;23:199–212. [PubMed: 14763437]
61. Galvan M, David JP, Delacourte A, Luna J, Mena R. Sequence of neurofibrillary changes in aging and Alzheimer's disease: A confocal study with phospho-tau antibody, AD2. J Alzheimers Dis 2001;3:417–425. [PubMed: 12214046]
62. Gray EG, Paula-Barbosa M, Roher A. Alzheimer's disease: paired helical filaments and cytomembranes. Neuropathol Appl Neurobiol 1987;13:91–110. [PubMed: 3614544]
63. Volk HA, Burkhardt K, Potschka H, Chen J, Becker A, Loscher W. Neuronal expression of the drug efflux transporter P-glycoprotein in the rat hippocampus after limbic seizures. Neuroscience 2004;123:751–759. [PubMed: 14706787]
64. Goedert M, Spillantini MG, Jakes R, Rutherford D, Crowther RA. Multiple isoforms of human microtubule-associated protein tau: sequences and localization in neurofibrillary tangles of Alzheimer's disease. Neuron 1989;3:519–526. [PubMed: 2484340]
65. Carmel G, Mager EM, Binder LI, Kuret J. The structural basis of monoclonal antibody Alz50's selectivity for Alzheimer's disease pathology. J Biol Chem 1996;271:32789–32795. [PubMed: 8955115]
66. LoPresti P, Szuchet S, Papasozomenos SC, Zinkowski RP, Binder LI. Functional implications for the microtubule-associated protein tau: localization in oligodendrocytes. Proc Natl Acad Sci U S A 1995;92:10369–10373. [PubMed: 7479786]
67. Espinoza M, de Silva R, Dickson DW, Davies P. Differential incorporation of tau isoforms in Alzheimer's disease. J Alzheimers Dis 2008;14:1–16. [PubMed: 18525123]
68. Necula M, Kuret J. Electron microscopy as a quantitative method for investigating tau fibrillization. Anal Biochem 2004;329:238–246. [PubMed: 15158482]
69. Duff K, Noble W, Gaynor K, Matsuoka Y. Organotypic slice cultures from transgenic mice as disease model systems. J Mol Neurosci 2002;19:317–320. [PubMed: 12540058]
70. Greenberg SG, Davies P. A preparation of Alzheimer paired helical filaments that displays distinct tau proteins by polyacrylamide gel electrophoresis. Proc Natl Acad Sci U S A 1990;87:5827–5831. [PubMed: 2116006]
71. O'Farrell PH. High resolution two-dimensional electrophoresis of proteins. J Biol Chem 1975;250:4007–4021. [PubMed: 236308]

Abbreviations used

AD
Alzheimer's disease

CNS
central nervous system

DLC
π-delocalized lipophilic cation

ODS
octadecyl sulfate

PARP1
Poly (ADP-ribose) polymerase-1

RIPA
radioimmunoprecipitation assay

SAR
structure-activity relationship

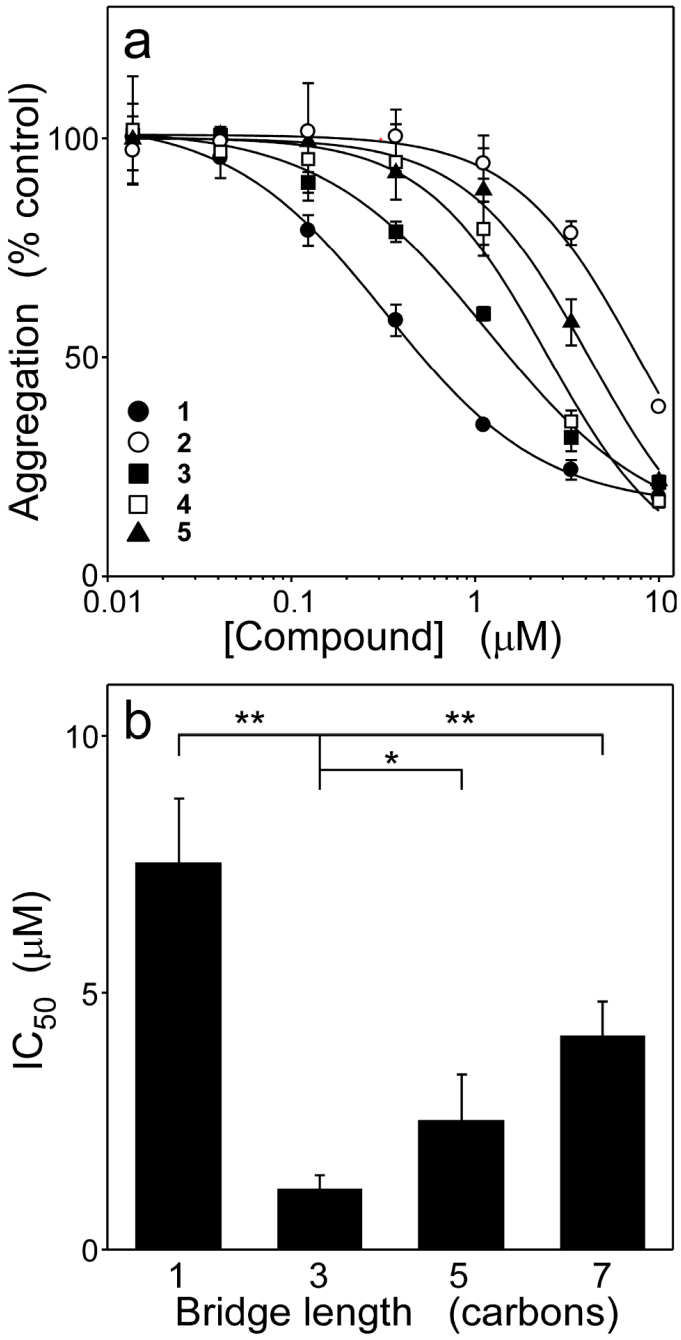

Figure 1. Polymethine bridge length modulates inhibitory activity

Tau protein (4 μM) was incubated with ODS (50 μM) without agitation (24 h at 37°C) in the presence of either thiacarbocyanines **1** - **5** or DMSO vehicle alone, then assayed for aggregation by filter trap assay. (a) Concentration dependence of inhibition, where each point represents aggregation expressed as a normalized percentage of aggregation measured in the presence of DMSO vehicle alone (triplicate determination ± SD), and each solid line represents best fit of the data points to eq 4. All tested compounds were active, but less so than lead compound **1**. (b) Replot of IC_{50} values determined in Panel (a) versus bridge length for compounds **2** - **5**. Inhibitory potency was maximal when the polymethine bridge consisted of three carbon atoms. *, $p < 0.05$; **, $p < 0.01$ when compared with compound **3** by Student's *t* test.

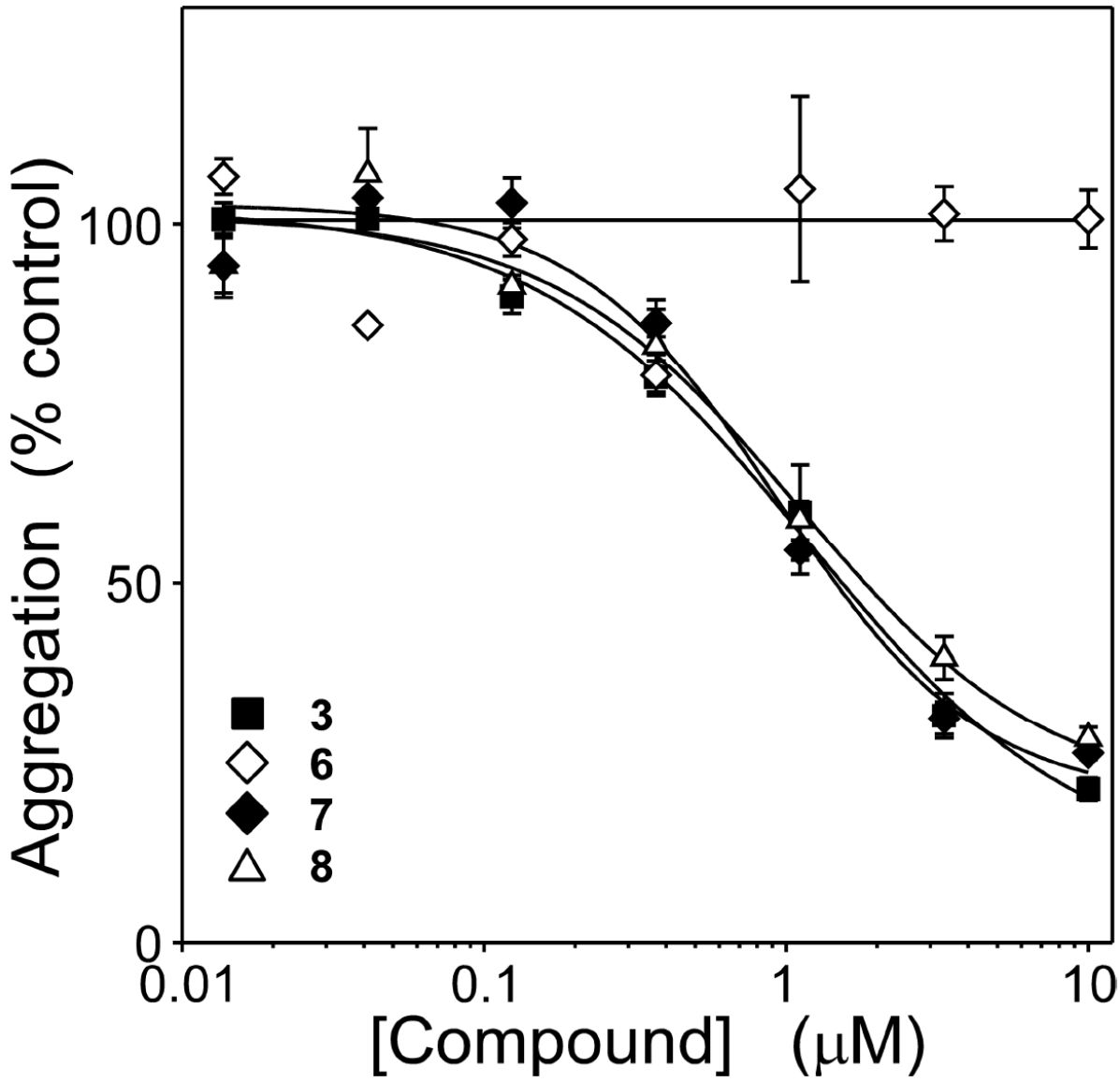

Figure 2. Multiple heterocycles support inhibitory activity

Tau protein (4 μM) was incubated with ODS (50 μM) without agitation (24 h at 37°C) in the presence of either **3, 6, 7, 8** (composed of benzothiazole, benzoxazole, quinoline, and dimethylindole heterocycles, respectively) or DMSO vehicle alone, then assayed for aggregation by filter trap assay. Each point represents normalized aggregation relative to the DMSO vehicle control (mean of triplicate determination ± SD), whereas each solid line represents best fit of the data points to eq 4. All heterocycles except benzoxazole supported inhibitory activity under these conditions.

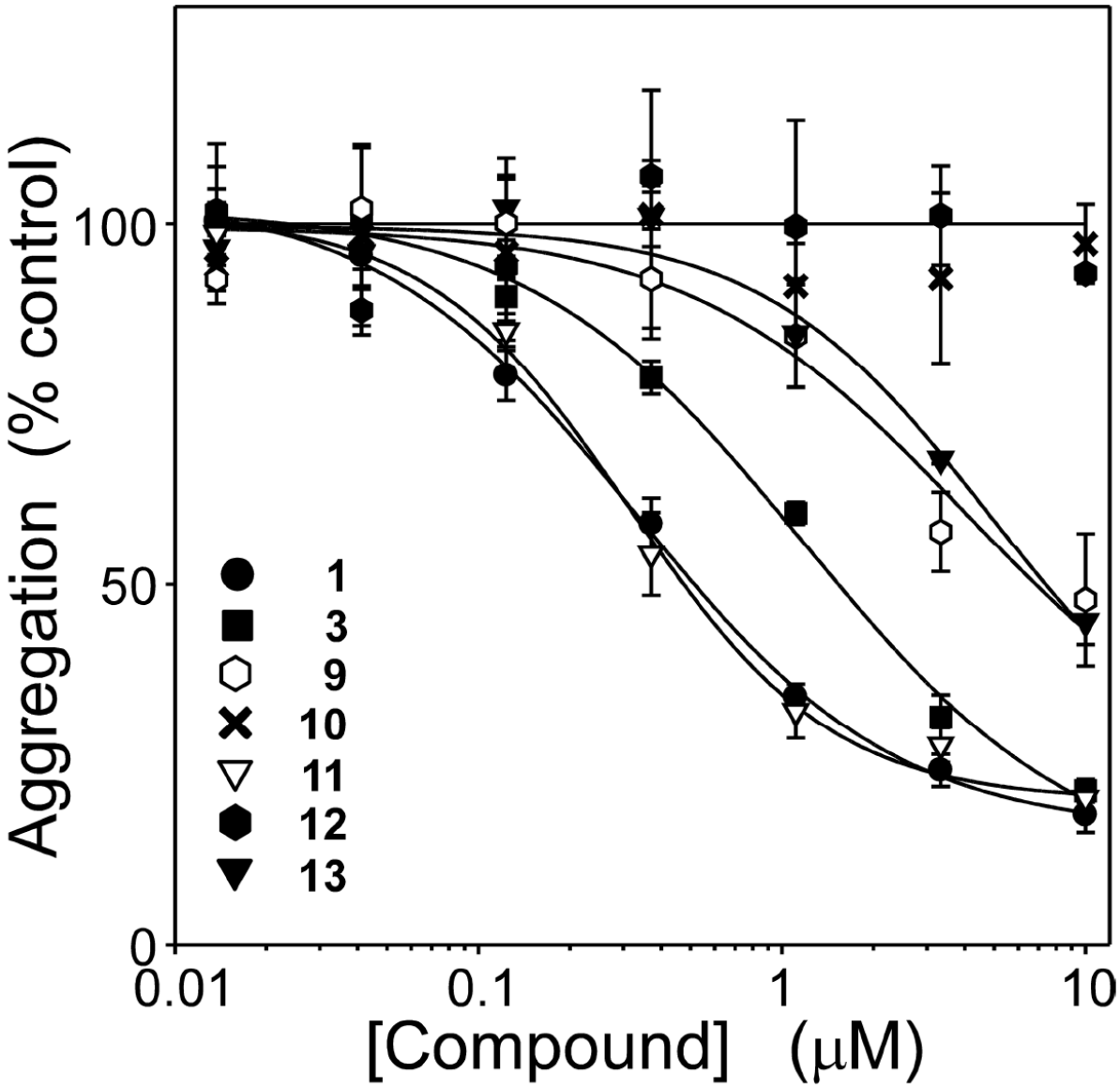

Figure 3. Meso- and N-substituents influence antagonist potency

Tau protein (4 μM) was incubated with ODS (50 μM) without agitation (24 h at 37°C) in the presence of either thiacarbocyanines **9** - **13** or DMSO vehicle alone, then assayed for aggregation by filter trap assay. Each point represents normalized aggregation relative to the DMSO vehicle control (mean of triplicate determination ± SD), whereas each solid line represents best fit of the data points to eq 4. Data for compounds **1** and **3** are replotted from Figure 1 for comparison. Extension of the N-substituent beyond two carbons decreased potency, whereas introduction of a methyl meso substituent increased potency. The combination of benzothiazole nucleus, three carbon bridge, methyl meso substituent, and ethyl N-substituents yielded an inhibitor (compound **11**) with the efficacy and potency of the starting compound 1, but with physicochemical properties more appropriate for biological experimentation.

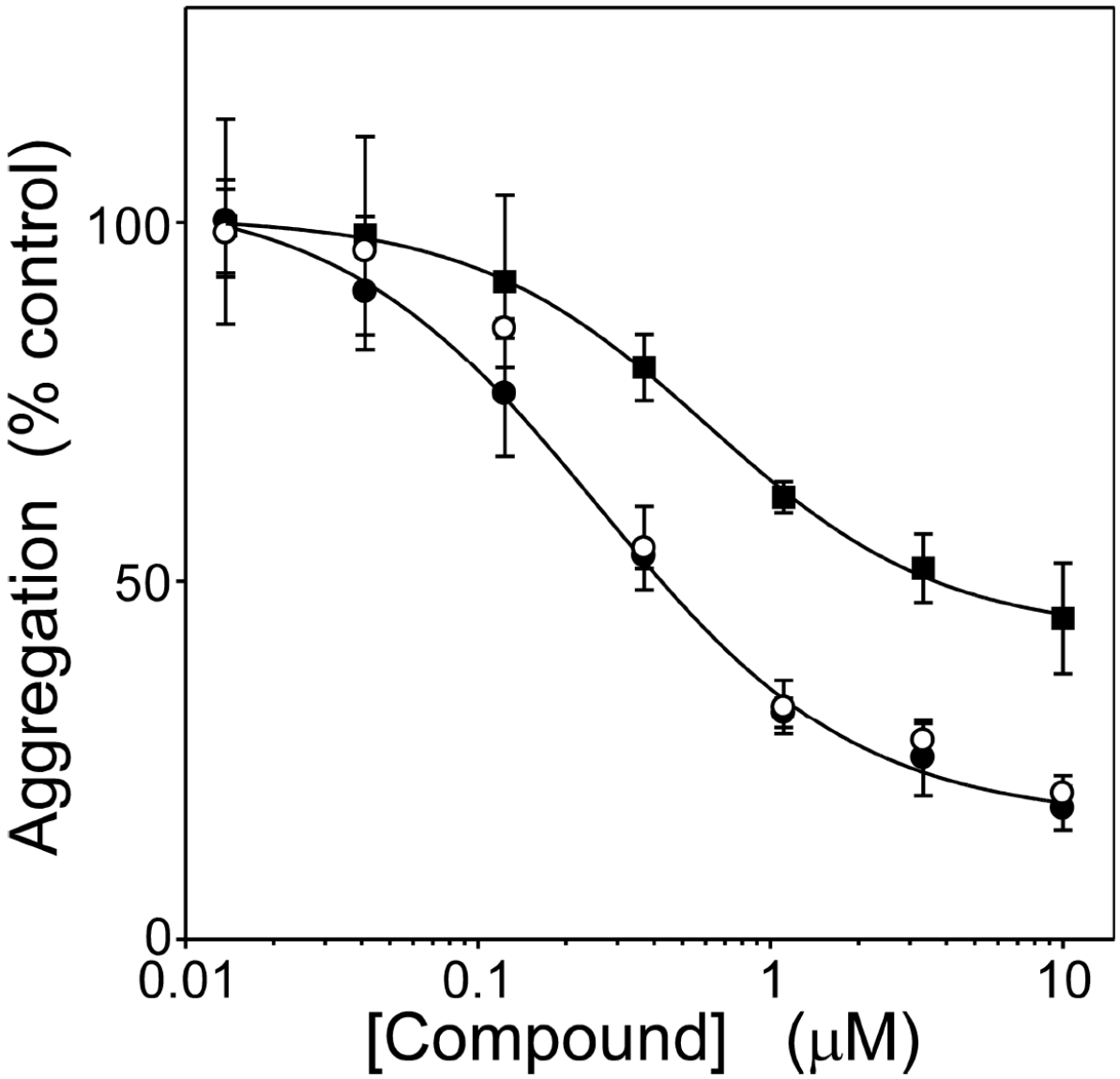

Figure 4. Thiacarbocyanine 11 is a stronger aggregation antagonist than Methylene blue

Tau protein (4 μM) was incubated with ODS (50 μM) without agitation (24 h at 37°C) in the presence of either **11**, Methylene blue, or DMSO vehicle alone, then assayed for aggregation. Each point represents normalized aggregation relative to the DMSO vehicle control (mean of triplicate determination ± SD), whereas each line represents best fit of the data points to eq 4. Compound **11** was equally efficacious when assayed by either filter trap assay (○) or direct measurement of total filament length by quantitative electron microscopy assays (●), confirming that inhibitory activity did not depend on assay modality. However, **11** was significantly more potent and efficacious than Methylene blue (■) (electron microscopy assay format).

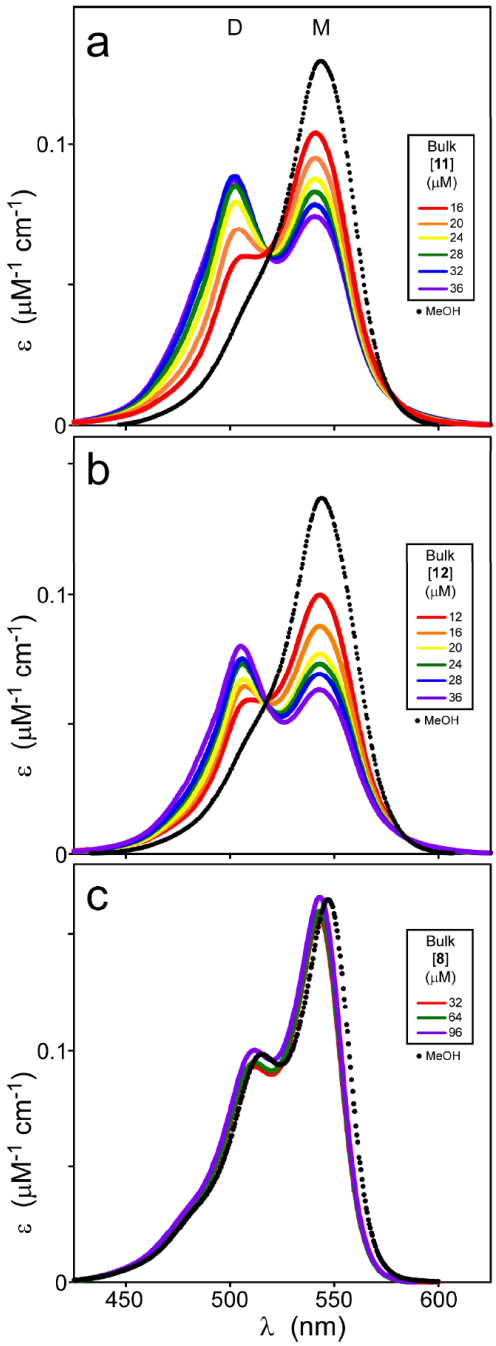

Figure 5. Inhibitory potency does not correlate with cyanine aggregation propensity

When dissolved in methanol at 5 μM concentration, compounds **11** (a), **12** (b), and **8** (c) yield simple spectra (dotted lines) consistent with monomeric structure (M). In assembly buffer (solid lines), increasing concentrations of compounds **11** and **12**, but not **8**, revealed the presence of both monomeric (M) and aggregated (D) species, with the latter more pronounced at high concentrations. These data suggest that **11** and **12**, but not **8**, underwent aggregation in aqueous solution at the concentrations tested.

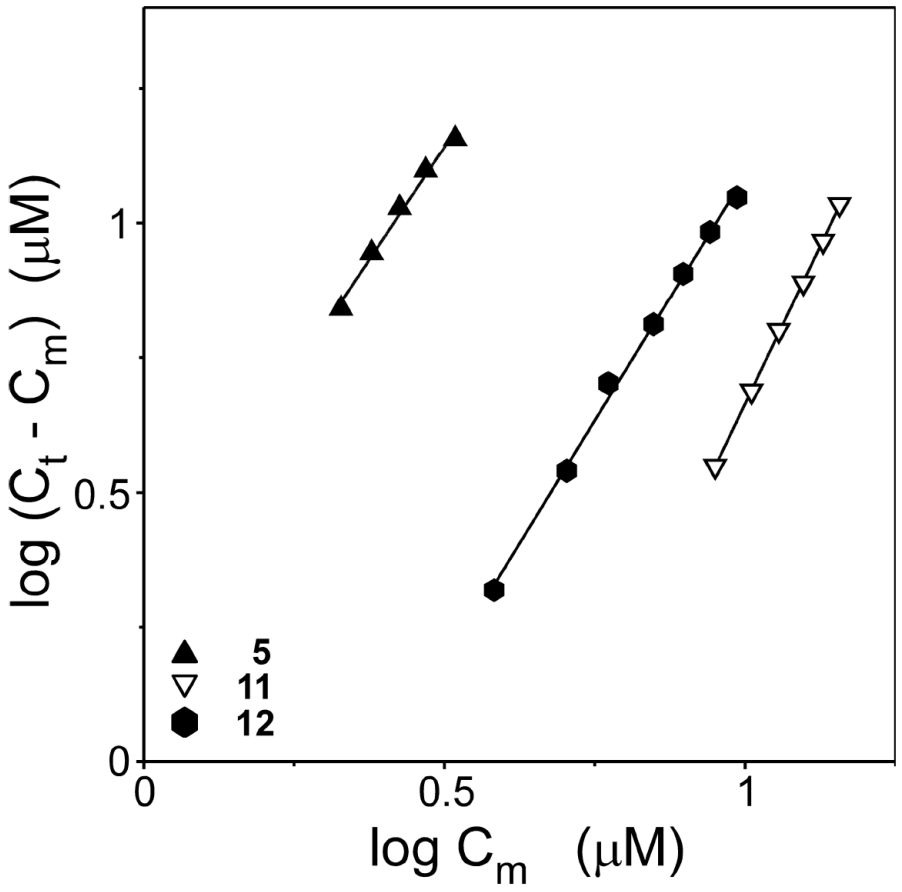

Figure 6. The principal cyanine aggregate formed in solution is a dimer

Concentrations of monomeric (C_m) and aggregate (C_t-C_m) forms of **11, 12**, and **5** were calculated from absorbance spectra and replotted on double logarithmic scales. Each point represents a spectrum collected at a different bulk compound concentration, whereas each line represents best fit of the data points to a linear regression. Regression slopes for **11, 12**, and **5** were 2.3 ± 0.1, 1.8 ± 0.1, and 1.7 ± 0.1, respectively, consistent with dimerization being mostly responsible for the spectral shifts of all three compounds.

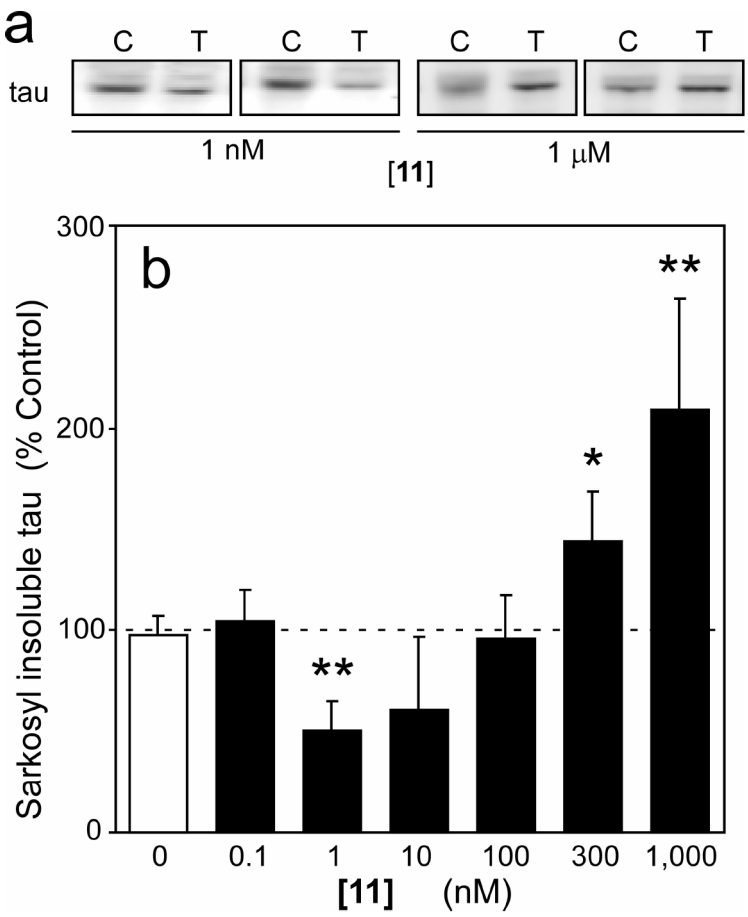

Figure 7. Compound 11 inhibits tau aggregation in organotypic slices

Slice cultures prepared from JNPL3 transgenic mice were incubated with either DMSO vehicle control or varying concentrations of **11** for seven days, then extracted and analyzed for levels of sarkosyl-insoluble tau (a measure of tau aggregation). (a) Two representative immunoblots collected after incubation with DMSO vehicle control (C) or thiacarbocyanine **11** (T) are shown. The presence of 1 nM **11** reduced the amount of tau aggregation in the slices relative to DMSO vehicle control, whereas 1 μM **11** exacerbated aggregation. (b) Sarkosyl-insoluble tau immunoreactivity was quantified by densitometry (n = three observations) and plotted as a normalized percentage of aggregation measured in the presence of DMSO vehicle alone. Tau aggregation was suppressed at **11** concentrations below 100 nM, but was aggravated at higher concentrations (≥300 nm). *, $p < 0.05$; **, $p < 0.01$ when compared to slices treated with vehicle alone by Student's t test.

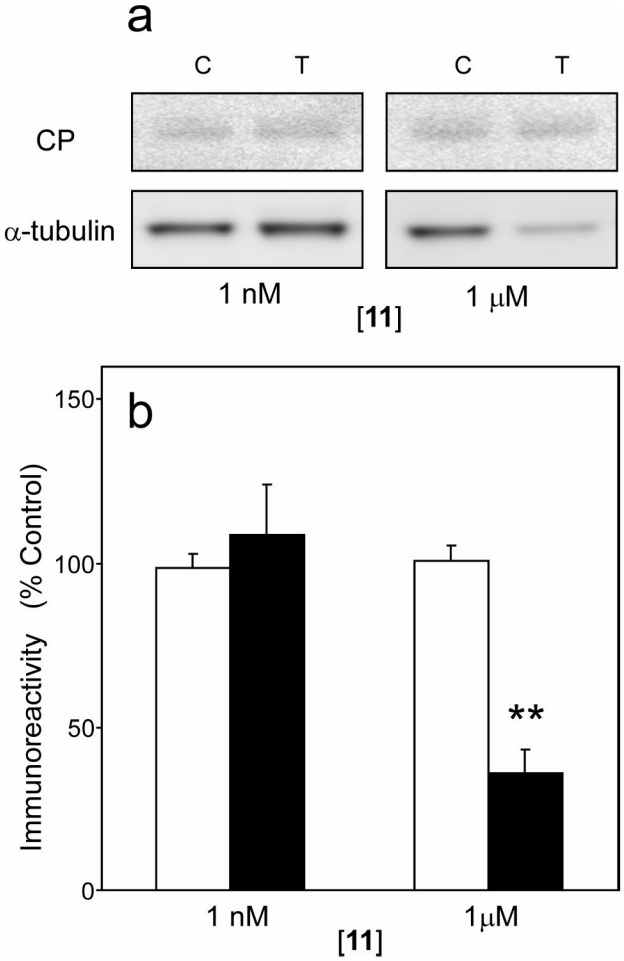

Figure 8. Compound 11 does not induce apoptosis in organotypic slices

Slices prepared from JNPL3 transgenic mice were incubated with either DMSO vehicle control or varying concentrations of **11** for seven days, then extracted and analyzed for levels of α-tubulin and cleaved PARP1. (a) Representative immunoblots collected after incubation with DMSO vehicle control (C) or **11** (T) are shown. (b) Levels of cleaved PARP1 (*hollow bar*) and α-tubulin (*solid bar*) immunoreactivity were quantified by densitometry (n = three observations) and plotted as a normalized percentage relative to treatment with vehicle alone. Cleaved PARP1 (CP) levels were unaffected after exposure to **11**, suggesting that executioner caspase activity was not activated even at the highest concentration tested. Similarly, efficacious concentrations of **11** (1 nM) did not modulate levels of α-tubulin immunoreactivity in tissue extracts. However, high concentrations of **11** associated with induction of tau aggregation (1 μM) led to marked decreases in α-tubulin immunoreactivity. *, $p < 0.05$; **, $p < 0.01$ when compared to slices treated with vehicle alone by Student's t test.

Table 1

Summary of molecular properties of cyanine salts used in SAR studies.

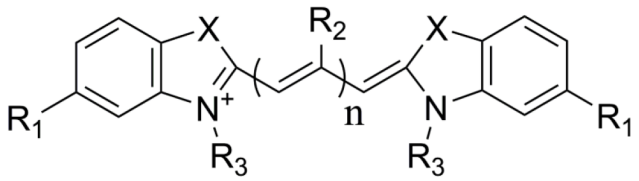

Y = counterion

Compd	X	n	R_1	R_2	R_3	Y	tPSA[a]	CLogP[a]	MW[b]	IC_{50} (μM)
1	S	1	$-OCH_3$	$-CH_2CH_3$	$-(CH_2)_2OH$	I^-	67.7	1.38	485.6	0.29 ± 0.02
2	S	0	H	---	$-CH_2CH_3$	I^-	8.8	1.94	339.5	~10[c]
3	S	1	H	H	$-CH_2CH_3$	I^-	8.8	2.52	365.5	0.96 ± 0.25
4	S	2	H	H	$-CH_2CH_3$	I^-	8.8	3.04	391.6	2.15 ± 0.47
5	S	3	H	H	$-CH_2CH_3$	I^-	8.8	3.56	417.6	5.00 ± 3.30[c]
6	O	1	H	H	$-CH_2CH_3$	I^-	35.1	1.24	333.4	≫10[c]
7	(CH=CH)	1	H	H	$-CH_2CH_3$	Cl^-	8.8	2.4	353.5	0.89 ± 0.20
8	$C(CH_3)_2$	1	H	H	$-CH_2CH_3$	I^-	6.2	3.52	385.6	0.98 ± 0.35
9	$C(CH_3)_2$	1	H	H	$-CH_2CH_2CH_3$	I^-	6.2	4.53	413.6	2.57 ± 1.06 [c]
10	S	1	H	H	$-(CH_2)_5CH_3$	I^-	8.8	6.67	477.7	≫10[c]
11	S	1	H	CH_3	$-CH_2CH_3$	I^-	8.8	3.07	379.6	0.28 ± 0.04
12	S	1	H	CH_3	$-(CH_2)_3SO_3^-$	*d*	123.2	-2.22	565.7	≫10[c]
13	S	1	*e*	CH_3	$-CH_2CH_3$	Br^-	8.8	5.39	479.7	3.29 ± 2.07[c]
14	$C(CH_3)_2$	3	*f*	H	$-(CH_2)_4SO_3^-$	Na^+	120.6	2.13	752.0	---

[a] tPSA and CLogP values were calculated from the website http://www.molinspiration.com/

[b] organic component of the salt.

[c] Accurate estimates of SE could not be determined owing to incomplete concentration-effect relationship.

[d] 1-ethylpyridinium.

[e] Naphthothiazole heterocyle

[f] Naphthoindole heterocycle.